Metallothionein Prevents Diabetes-Induced Deficits in Cardiomyocytes by Inhibiting Reactive Oxygen Species Production

Gang Ye,[1] Naira S. Metreveli,[1] Jun Ren,[2] and Paul N. Epstein[1]

Many individuals with diabetes experience impaired cardiac contractility that cannot be explained by hypertension and atherosclerosis. This cardiomyopathy may be due to either organ-based damage, such as fibrosis, or to direct damage to cardiomyocytes. Reactive oxygen species (ROS) have been proposed to contribute to such damage. To address these hypotheses, we examined contractility, Ca^{2+} handling, and ROS levels in individual cardiomyocytes isolated from control hearts, diabetic OVE26 hearts, and diabetic hearts overexpressing antioxidant protein metallothionein (MT). Our data showed that diabetic myocytes exhibited significantly reduced peak shortening, prolonged duration of shortening/relengthening, and decreased maximal velocities of shortening/relengthening as well as slowed intracellular Ca^{2+} decay compared with control myocytes. Overexpressing MT prevented these defects induced by diabetes. In addition, high glucose and angiotensin II promoted significantly increased generation of ROS in diabetic cardiomyocytes. Chronic overexpression of MT or acute in vitro treatment with the flavoprotein inhibitor diphenyleneiodonium or the angiotensin II type I receptor antagonist losartan eliminated excess ROS production in diabetic cardiomyocytes. These data show that diabetes induces damage at the level of individual myocyte. Damage can be attributed to ROS production, and diabetes increases ROS production via angiotensin II and flavoprotein enzyme–dependent pathways. _Diabetes_ 52:777–783, 2003

Diabetes is a major risk factor for the development of congestive heart failure (1). Diabetic cardiomyopathy, a diabetes-related myopathic state and a major cause of disability and morbidity for patients with diabetes, has been documented to lead to congestive heart failure even in the absence of any other risk factors such as hypertension or coronary artery disease, suggesting that diabetic cardiomyopathy is a specific cardiomyopathy associated with diabetes and independent of macrovascular complications. Results from chemically induced insulinopenic (2) as well as in genetically predisposed insulin-resistant (3) rodent models (4) and human histological (5) and clinical observations (6) provide support for this concept of a specific diabetic cardiomyopathy, although its mechanism remains poorly understood. The hallmarks of diabetic cardiomyopathy, in experimental or clinical settings, include prolongation of contraction and relaxation, compromised relaxation velocity, and impaired contractility (3,4).

Reactive oxygen species (ROS), such as the superoxide radical, the hydroxyl radical, and H_2O_2, are continuously produced in most cells under physiological conditions, and their levels are regulated by a number of enzymes and physiological antioxidants such as superoxide dismutase, glutathione peroxidase, and catalase as well as by other nonenzymatic antioxidants. However, when the production of ROS becomes excessive, oxidative stress will develop and impose a harmful effect on the functional integrity of biological tissue. There is convincing experimental and clinical evidence that the generation of ROS is increased in both types of diabetes and that the onset of diabetes and its complications, including diabetic cardiomyopathy, are closely associated with oxidative stress (7,8).

Metallothionein (MT) is a cysteine-rich protein that can bind heavy metal ions such as copper and zinc (9). It also has a strong effect in scavenging free radicals because of its high thiol content (10). The concept is supported by the fact that MT can scavenge hydroxyl radicals in vitro (11) and provide protection against radiation damage (12). Also, some chemicals that stimulate the production of ROS can increase MT levels (13). However, it was observed that MT in the heart of adult rodents was the lowest of any organs when compared with the liver, kidney, small intestine, testes, and brain (14), indicating that the heart tissue may be susceptible to oxidative stress as a result of low antioxidant defense (15). To address whether increased ROS is involved in the pathogenesis of diabetic cardiomyopathy and the potential protection of MT against harmful effects of ROS in the development of diabetic cardiomyopathy, we used a transgenic line that overexpresses MT specifically in the heart from the α-myosin heavy chain promoter. MT transgenic mice were crossbred with OVE26 diabetic mice, and the offspring were used for study. In a previous report, we demon-
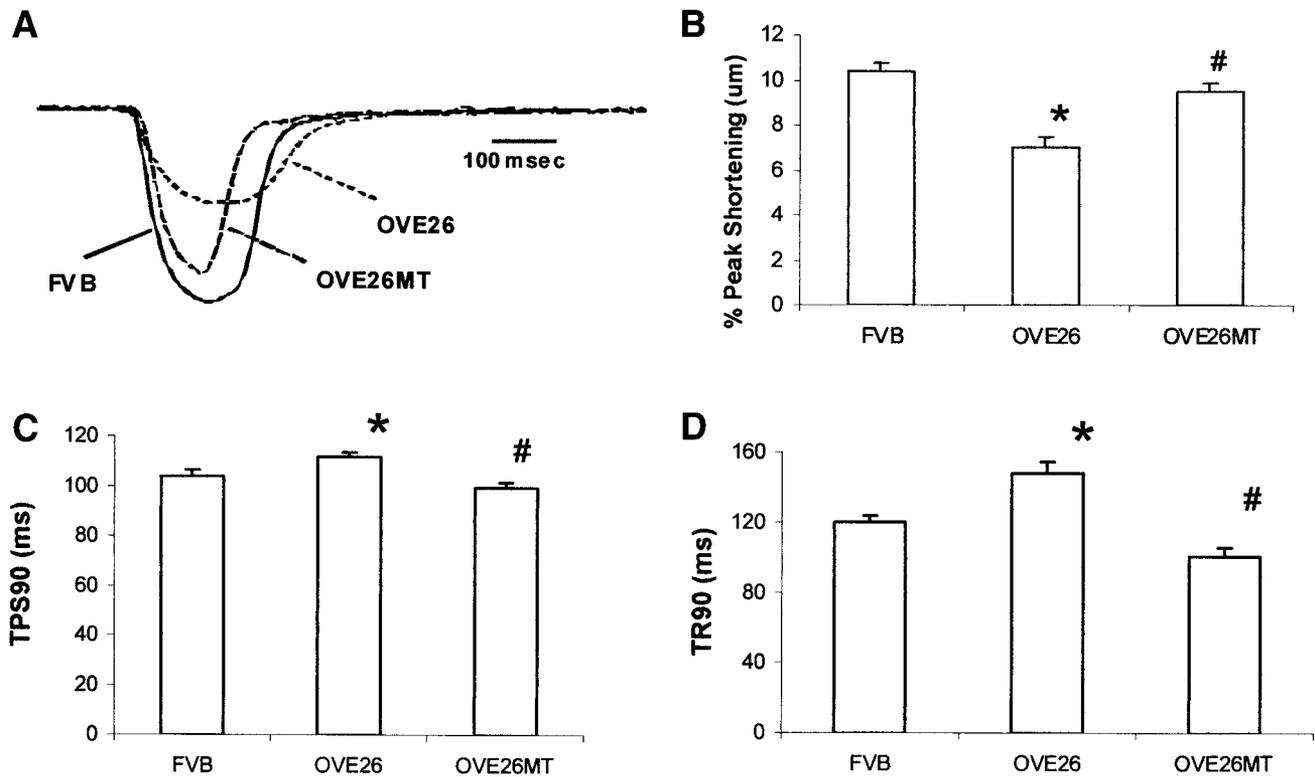
FIG. 1. Reduced contractility in diabetic cardiomyocytes and protection by overexpression of MT. Contractile properties of ventricular myocytes isolated from wild-type (FVB), OVE26 diabetic, and OVE26 crossed to OVE26MT mouse hearts. Representative cell shortening traces (*A*), PS amplitude (*B*), TPS$_{90}$ (*C*), and TR$_{90}$ (*D*). Mean ± SE, *n* = 60 cells/group, six mice/group. *P < 0.01 vs. FVB group; #P < 0.01 vs. OVE26 group.

strated that MT benefits diabetic heart morphology and whole-heart ischemic contractility (16). In the current study, we show that MT protection of mechanical performance and calcium metabolism is exerted at the level of the individual ventricular myocyte. We also found that prolonged diabetes increases cardiomyocyte ROS production in response to angiotensin II and high glucose and that MT overexpression prevents this damaging response of the heart to diabetes.

RESEARCH DESIGN AND METHODS

Animals. OVE26 diabetic mice have been previously described (17). MT mice that overexpress MT 10-fold in the heart were also previously described (18). Transgenic mice of both lines were identified by the presence of phenotypic markers. OVE26-positive mice were recognized by the presence of small eyes as a result of the co-integration of the GR19 gene, which is expressed in the eye. MT-positive mice were recognized by the presence of coat color as a result of co-integration of the tyrosinase gene that corrects the mutant tyrosinase gene of FVB mice (19). Age-matched OVE26, OVE26MT, and FVB mice of both sexes were obtained at 20 weeks of age. All transgenic and nontransgenic animals were maintained on the inbred FVB background. Mice were maintained on a 12-h light/dark cycle and received food (Purina Laboratory Rodent Diet 5001) and water ad libitum. Serum triglycerides were measured with a Sigma triglyceride (UV) kit. The U.S. Department of Agriculture certified institutional animal care committee approved all animal procedures.

Isolation of ventricular myocytes. Single ventricularmyocytes were isolated by enzymatic dissociation with collagenase II (Worthington, NJ) from adult mice by modification of described procedures (4). Briefly, animals received an injection of heparin (1,000 units/kg, i.p.) and were anesthetized with ketamine (150 mg/kg, i.p.) and xylazine (22.5 mg/kg, i.p.). Their hearts were rapidly removed and perfused (at 37°C) with oxygenated (5% CO_2/95% O_2) Krebs-Henseleit (KH) calcium-free buffer (in mmol: 135 NaCl, 4.0 KCl, 1.0 $MgCl_2$, 0.33 NaH_2PO_4, 10 HEPES and glucose, and 10 Butanedione [pH 7.4]). Hearts were then perfused with the same Ca^{2+}-free KH buffer with collagenase II (0.9 mg/ml) for 15–20 min until the heart became flaccid. After

perfusion, the left ventricle was removed, minced, and resuspended with same Ca^{2+}-free KH at room temperature. Extracellular Ca^{2+} was added incrementally back to 1.2 mmol/l. Isolated myocytes were maintained at room temperature in a serum-free medium consisting of medium 199 (GIBCO) with Hanks' salts containing 25 mmol HEPES for additional mechanical and fluorescent studies. Mechanical properties remained relatively stable in myocytes for 8–10 h in the serum-free medium. Cell yield was ~50–70%. There was no notable difference of yield between normal FVB and transgenic mice. Myocytes with obvious sarcolemmal blebs or spontaneous contractions were not used. Only rod-shaped myocytes with clear edges were used for recording of mechanical properties, intracellular Ca^{2+} transients, and ROS fluorescent measurement.

Cell shortening/relengthening. Mechanical properties of ventricular myocytes were assessed using a video-based edge-detection system (IonOptix, Milton, MA) (4). Cells were placed in a Teflon glass coverslip dish (Harvard Apparatus, Holliston, MA) mounted on the stage of an inverted microscope (Olympus, IX-70). The cells were field-stimulated at a frequency of 1.0 Hz, 4-ms duration, using a pair of platinum wires placed on opposite sides of the dish chamber connected to the MyoPacer Field Stimulator (IonOptix). The polarity of the stimulatory electrodes was reversed frequently to avoid possible build-up of electrolyte by-products. The myocytes being studied were displayed on the computer monitor using an IonOptix MyoCam camera, which rapidly scans the image area every 8.3 ms such that the amplitude and velocity of shortening/relengthening was recorded with good fidelity. The soft-edge software (IonOptix) was used to capture changes in cell length during shortening and relengthening. Cell shortening and relengthening were assessed using the following indexes: peak shortening (PS), time to 90% PS (TPS$_{90}$), time to 90% relengthening (TR$_{90}$), and maximal velocities of shortening and relengthening (±dL/dt).

Intracellular fluorescence measurement of Ca^{2+}. A separate cohort of myocytes was loaded with fura-2/AM (1.0 μmol/l) for 30 min, and fluorescence measurements were recorded with a dual-excitation fluorescence photomultiplier system (IonOptix). Myocytes were placed in a dish chamber on the stage of an Olympus IX-70 inverted microscope and imaged through a Fluor 100× oil objective. Cells were exposed to light emitted by a 75-W lamp and passed through either a 360- or a 380-nm filter (bandwidths were ±15 nm), while being stimulated to contract at 1.0 Hz. Fluorescence emissions were detected between 480 and 520 nm by a photomultiplier tube after first

illuminating the cells at 360 nm for 0.5 s then at 380 nm for the duration of the recording protocol (333 Hz sampling rate). The 360-nm excitation scan was repeated at the end of the protocol, and qualitative changes in intracellular Ca^{2+} concentration ($[Ca^{2+}]_i$) were inferred from the ratio. Intracellular Ca^{2+} transients were measured as changes in fura2 fluorescence intensity (FFI). ΔFFI was determined as the difference between the levels of Ca^{2+} in the systolic and diastolic conditions (ΔFFI = peak FFI − baseline FFI). The time course of the fluorescence signal decay (τ: the duration where Ca^{2+} transient decays 67% from the peak level) was calculated to assess intracellular Ca^{2+} clearing rate.

Intracellular fluorescence measurement of ROS. The membrane-permeable probe 5-(6)-chloromethyl-2′, 7′-dichlorodihydrofluorescein diacetate (CM-H2DCFDA) enters cardiomyocytes and produces a fluorescent signal after intracellular oxidation by ROS such as hydrogen peroxide and hydroxyl radical (20). Intracellular oxidant stress was monitored by measuring changes in fluorescence resulting from intracellular probe oxidation. Isolated myocytes were loaded with 1 μmol/l CM-H2DCFDA (Molecular Probes, Eugene, OR) for 30 min. After myocytes were washed, fluorescence intensity from individual cells was measured using an excitation wavelength of 485 nm and an emission wavelength of 530 nm. Cells were sampled at random in each preparation using an Olympus IX70 inverted microscope equipped with a digital cooled charged-coupled device camera and ImagePro image analysis software (Media Cybernetics, Silver Spring, MD). Fluorescence was calibrated with InSpeck microspheres (Molecular Probes). Calibration curves were generated, and cell brightness was measured. The InSpeck microspheres were used as internal standards. The intensities of cells and beads were calibrated by subtraction of the background, and the final result for comparison was assessed by ratio of myocyte fluorescent intensities divided by intensities of internal fluorescent beads. The cardiomyocytes from each group were incubated at room temperature separately in M199 medium with normal glucose concentration as control (5.5 mmol/l), high glucose (25 mmol/l), normal glucose plus angiotensin II (50 mmol/l), and normal glucose plus hydrogen peroxide as a positive control (H_2O_2, 40 μmol/l). Some incubations included 1 μmol/l diphenyleneiodonium (DPI) or 0.1 μmol/l losartan. The different culture conditions were begun 30 min before CM-H2DCFDA was added to the medium. After 30 min of incubation of CM-H2DCFDA, the myocytes were washed twice and images were captured by Olympus IX70 inverted microscope equipped with a charged-coupled device camera. For results in Fig. 5, images were captured from live cells. For results in Fig. 6, myocytes were fixed in 4% paraformaldehyde after incubation and stored at 4°C for up to 16 h before imaging. There were 100 cells in each group.

Data analysis. Data are expressed as means ± SE. Statistical comparisons were performed by ANOVA and Student-Newman-Keuls post hoc tests among different groups. Significance was defined as $P < 0.05$.

RESULTS

Cell shortening and relengthening in ventricular myocytes from FVB, OVE26, and OVE26MT mice. Similar rod-shaped cardiomyocytes with good striation and edges were obtained from FVB, OVE26, and OVE26MT mice. The averaged resting myocyte length was not significantly different among the two transgenic and the wild-type mouse groups (OVE26 113.13 ± 2.83 μm, OVE26MT 118.44 ± 2.72 μm, and FVB 121.09 ± 3.04 μm). As shown in Figs. 1 and 2, cardiomyocyte contractile function from OVE26 mice was markedly depressed. The cardiomyocytes from OVE26 mice showed significantly reduced peak shortening (OVE26 versus FVB, $P < 0.01$; Fig. 3B) and ±dL/dt$_{max}$ (OVE26 versus FVB, $P < 0.01$; Fig. 2A and B) as compared with those from FVB mice. Myocytes from OVE26 mice also exhibited significantly prolonged TPS$_{90}$ (OVE26 versus FVB, $P < 0.05$; Fig. 1C) and TR$_{90}$ (OVE26 versus FVB, $P < 0.01$; Fig. 1D). Overexpressed MT in the heart significantly reversed the impaired myocyte contractile performance (PS, Fig. 1B; ±dL/dt$_{max}$, Fig. 2A and B) and prolongation of myocyte contraction and relengthening (TPS$_{90}$ and TR$_{90}$, Fig. 1C and D) by diabetes (OVE26MT versus OVE26, $P < 0.01$). The benefits provided by MT overexpression occurred despite the fact that MT does not reduce diabetic blood glucose, as we previously reported
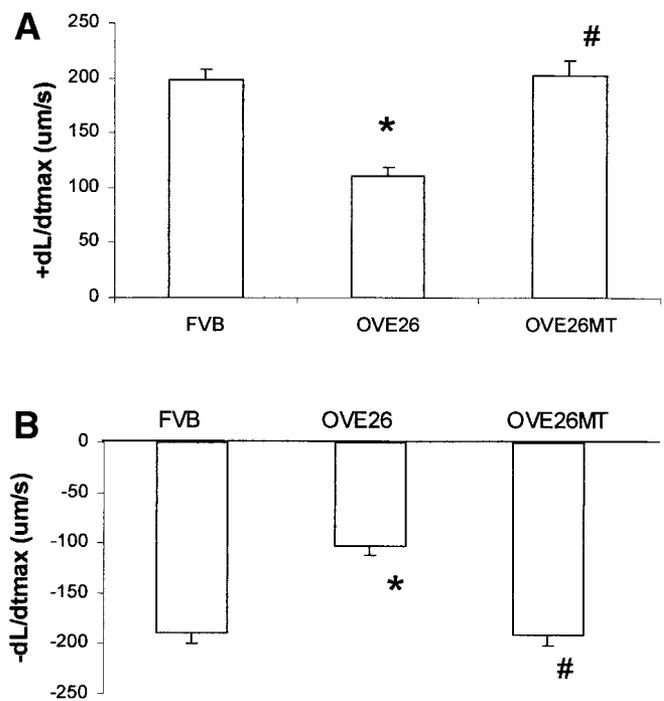
FIG. 2. Slow contraction and relaxation rates in OVE26 but not in OVE26MT cardiomyocytes. Maximal velocities of cell shortening (+dL/dt; A) and relengthening (-dL/dt; B) in ventricular myocytes isolated from FVB, OVE26 diabetic, and OVE26MT mouse hearts. Mean ± SE, n = 60 cells/group, six mice/group. *P < 0.01 vs. FVB group; #P < 0.01 vs. OVE26 group.

(16), or elevated serum triglyceride levels (OVE26 349.9 ± 62.9, OVE26MT 467.7 ± 29.5, and FVB 107.6 ± 7.7, $P < 0.001$ for FVB versus both other groups by ANOVA and Bonferroni test).

Intracellular Ca^{2+} transient in ventricular myocytes from FVB, OVE26, and OVE26MT mice. Myocytes from the three groups exhibited similar peak and baseline FFI (data not shown) and no differences of ΔFFI (Fig. 3B). As shown in Fig. 3C, recovery of the Ca^{2+} transient occurred more rapidly in control FVB cardiomyocytes than in OVE26 myocytes (τ, FVB 178.78 ± 8.77 ms vs. OVE26 261.97 ± 14.23; $P < 0.01$). However, overexpressed MT significantly facilitated the calcium-clearing rate in diabetic cardiomyocytes (OVE26MT 190.34 ± 10.26 ms vs. OVE26 261.97 ± 14.23 ms; $P < 0.01$).

Intracellular ROS levels in ventricular myocytes from FVB, OVE26, and OVE26MT mice. Figures 4 and 5 show ROS production measured with CM-H2DCFDA. Normal extracellular glucose produced similar ROS intensities among the cardiomyocytes from all three groups. After exposure of myocytes to 40 μmol/l H_2O_2, the fluorescent intensities were significantly increased in the cardiomyocytes from the three groups compared with normal glucose incubation, but there were no significant differences among the three groups. Treatment of myocytes with high glucose (25 mmol/l) or angiotensin II (50 nmol/l) for 60 min did not affect the ROS level in control cardiomyocytes but caused a significantly increased ROS in the OVE26 cardiomyocytes compared with those in the normal condition of glucose (OVE26 HG versus OVE26 NG, $P < 0.001$). However, the effects of high glucose or angiotensin II on ROS production were completely abolished by overexpressed MT (OVE26MT versus OVE26, $P < 0.001$).
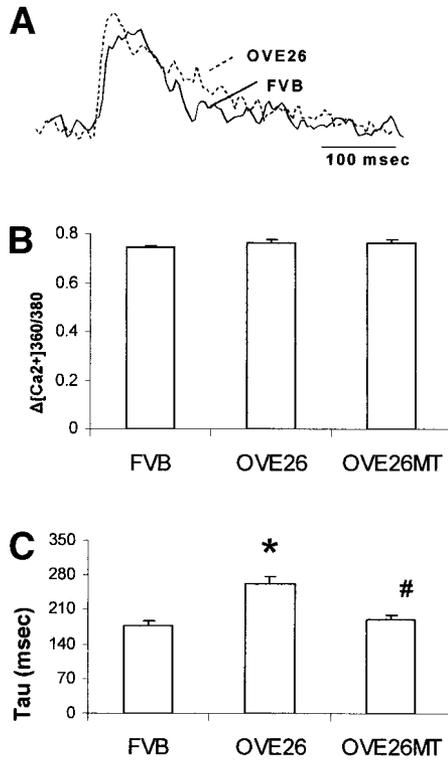
FIG. 3. There is no difference in $\Delta[Ca^{2+}]360/380$ ratio, but Ca^{2+} decay time is extended in OVE26 but not in OVE26MT cardiomyocytes. Intracellular Ca^{2+} properties in ventricular myocytes from FVB, OVE26 diabetic, and OVE26MT mouse hearts. A: Typical intracellular Ca^{2+} transients from FVB and OVE26 groups. B: $\Delta[Ca^{2+}]360/380$ ratio in myocyte from FVB, OVE26, and OVE26MT mouse hearts. C: Intracellular Ca^{2+} transient decay rate (τ) in myocytes from FVB, OVE26, and OVE26MT mouse hearts. Mean $\pm$ SE, $n = 60$ cells/group, six mice/group. $*P < 0.01$ vs. FVB group; $\#P < 0.01$ vs. OVE26 group.

FIG. 4. Representative cardiomyocytes after incubation with CM-H_2DCFDA for 30 min. A: Myocyte in M199 medium. B: Myocyte in M199 medium treated with H_2O_2 (40 µmol/l).

To ascertain the source of increased ROS in diabetic cells, we incubated OVE26 and FVB myocytes with 10 µmol/l DPI and 0.1 µmol/l losartan. DPI is an inhibitor of flavoprotein-containing enzymes, including NADPH oxidase. Losartan is a specific angiotensin II type I receptor antagonist. As shown in Fig. 6, both DPI and losartan eliminated the increased fluorescence induced in OVE26 myocytes by either angiotensin II or high glucose. These inhibitors had no significant effect on fluorescence in FVB myocytes.

DISCUSSION

This is the first study to evaluate the efficacy of permanent antioxidant protection of individual cardiomyocytes from diabetes. These studies were carried out in myocytes from the OVE26 mouse. Although this model has not been widely used to study diabetes complications, it provides several advantages: all OVE26 mice have a very consistent onset and severity of diabetes, their duration of diabetes is long, they can live with hyperglycemia for 2 years without insulin therapy, and specific damage to the β-cell occurs without use of toxic drugs. Diabetes is produced in heterozygous OVE26 animals, allowing these mice to be cross-bred easily to other strains of mice (16).

OVE26 diabetic cardiomyocytes had reduced contractility and prolonged calcium transients. The amplitude of cell shortening was decreased, the duration of contraction was increased, and the rates of contraction and relaxation
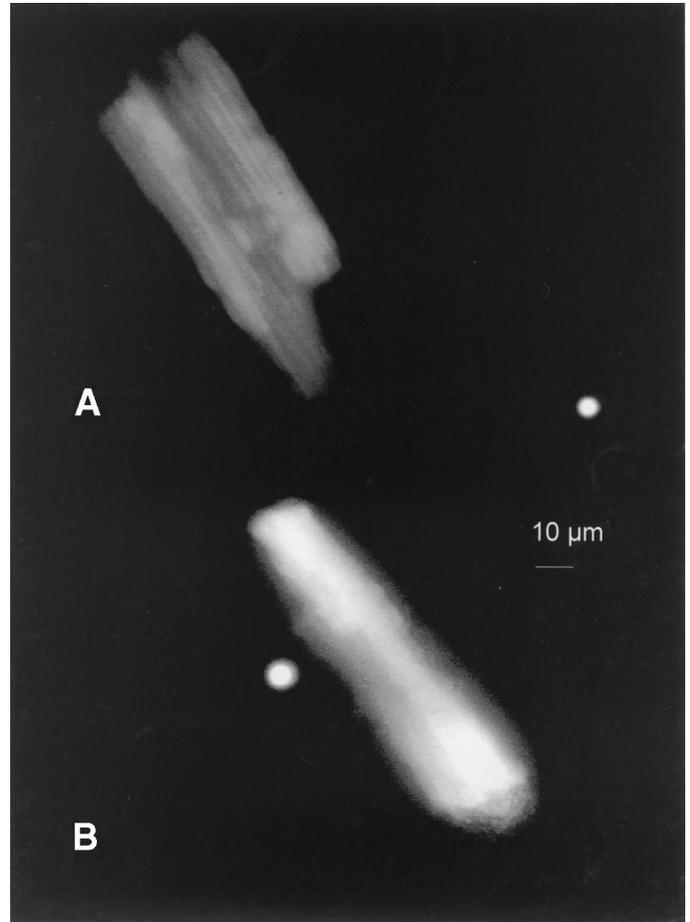
were reduced. This demonstrates that the impaired contractility of the intact diabetic heart is due to defects in the individual myocyte, rather than just increased cardiac fibrosis. These results are in agreement with data obtained in other models of diabetes (21,22) and confirm the validity of the OVE26 model.
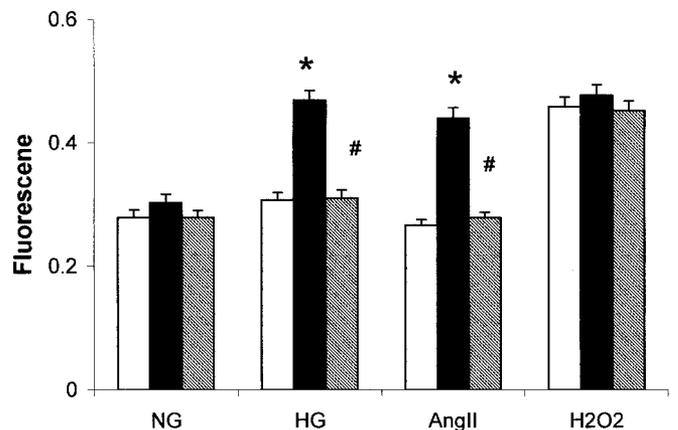

FIG. 5. ROS changes after exposure of cardiomyocytes from FVB (☐), OVE26 (■), and OVE26MT (▨) mice to high glucose, angiotensin II, and H_2O_2. $*P < 0.001$ vs. FVB; $\#P < 0.001$ vs. OVE26MT. NG, normal glucose (5.5 mmol/l); HG, high glucose (25 mmol/l); AngII, 5.5 mmol/l glucose + angiotensin II (50 nmol/l); H_2O_2, 5.5 mmol/l glucose + hydrogen peroxide (40 µmol/l).
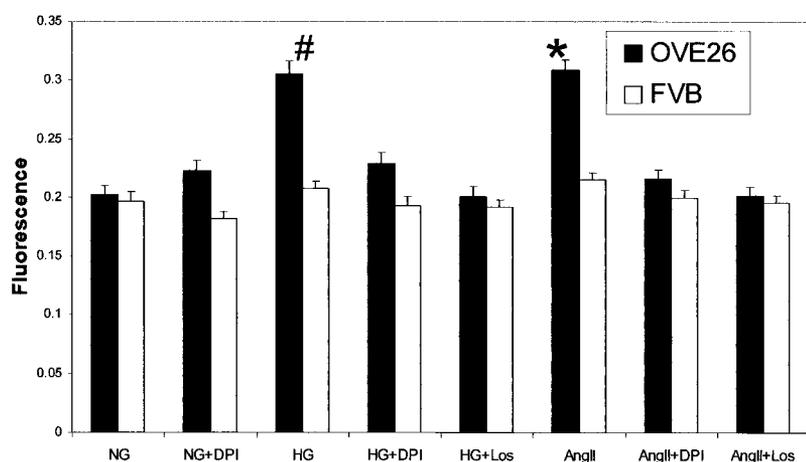
FIG. 6. DPI and losartan block high glucose and angiotensin II stimulated ROS production in OVE26 cardiomyocytes. *$P < 0.001$ vs. all other values except OVE26 with high glucose; #$P < 0.001$ vs. all other values except OVE26 with angiotensin II. NG, normal glucose (5.5 mmol/l); NG+DPI, 5.5 mmol/l glucose and 1 μmol/l DPI; HG, high glucose (25 mmol/l); HG+DPI, 25 mmol/l glucose and 1 μmol/l DPI; HG+losartan, 25 mmol/l glucose and 0.1 μmol/l mmol/l losartan; AngII, 5.5 mmol/l glucose + 50 nmol/l angiotensin II; Ang II+DPI, 5.5 mmol/l glucose and 50 nmol/l angiotensin II and 1 μmol/l DPI.

Calcium transients in diabetic cardiomyocytes were also abnormal. As seen in other diabetic models (22), decay of intracellular Ca^{2+} transients in OVE26 myocytes was significantly slowed. The slow Ca^{2+} clearing is consistent with and may be the cause of the prolonged duration of myocyte relengthening. Slow relengthening is a hallmark of diabetic cardiomyopathy. In contrast to decay rate, resting and peak Ca^{2+} levels were similar between the control and diabetic cardiomyocytes. Reports regarding intracellular Ca^{2+} level in diabetic cardiomyocytes are somewhat controversial. Early studies reported an increase in resting Ca^{2+} (23), whereas Noda et al. (24) reported a reduced basal Ca^{2+} in diabetic cardiomyocytes. Several reports demonstrated no differences in basal Ca^{2+} or peak Ca^{2+} levels between diabetic and control cardiomyocytes (25–27), which is consistent with our results. Therefore, there may not be significant alteration of Ca^{2+} levels that correspond to the depressed contraction in diabetic cardiomyocytes. Attenuated calcium sensitivity of the contractile apparatus or changes in cardiac contractile proteins may be more important than absolute Ca^{2+} levels to the reduced shortening of diabetic cardiomyocytes (28).

Many studies report that diabetic hearts exhibit characteristics of oxidative stress. OVE26 hearts have increased levels of oxidized glutathione (16), and hearts of BB (29) and streptozotocin (30) diabetic rats show induction of antioxidant enzymes. This ROS stress of diabetes can produce oxidative damage including lipid peroxidation (31,32) and nitrotyrosine formation (20). To determine whether oxidative stress was a cause or consequence of diabetic cardiomyopathy, we placed the cardiac transgene for the antioxidant protein MT on the OVE26 background (16). MT overexpression was remarkably effective in ameliorating functional deficits in OVE26 diabetic cardiomyocytes, despite that MT overexpression in no way reduced the exposure of cardiomyocytes to the severe hyperglycemic environment in these mice. MT overexpression completely reversed diabetes-induced diminished PS amplitude, prolonged duration and reduced maximal velocities of contraction and relaxation, and the slower intracellular Ca^{2+} transient decay. This indicates that ROS is essential to the pathogenesis of diabetic cardiomyopathy. Our preliminary data showing that two other antioxidant transgenes (unpublished results) protect from OVE26 diabetic cardiomyopathy confirm that it was the antioxidant actions of MT that protected the diabetic heart.

Increased oxidative damage suggests elevated ROS production in diabetic cardiomyocytes. Consistent with this, OVE26 myocytes produced more ROS in the presence of angiotensin II than myocytes from control mice or mice protected by the MT transgene. Bendall et al. (33) recently showed that angiotensin II stimulates cardiac NADPH oxidase, an enzyme that produces superoxide at the expense of the electron donor NADPH. Losartan blocked the response to angiotensin II in OVE26 myocytes. Consistent with a possible role for NADPH oxidase DPI, an inhibitor of flavoprotein enzymes such as NADPH oxidase blocked excess ROS production produced by angiotensin II.

High glucose also stimulated ROS production in OVE26 myocytes. Several sources have been proposed for enhanced ROS formation in hyperglycemia. These include mitochondrial electron transport, NADPH oxidase, and autoxidation of glucose. Mitochondria are the major source of ROS in most cells as a result of superoxide-generating electron-transport intermediates such as ubisemiquinone. Increased substrate for electron transport increases the mitochondrial membrane potential, which results in increased ROS production (34). The Brownlee laboratory has shown that hyperglycemia increases electron transport–generated superoxide in endothelial cells, which activates several pathways thought to lead to complications of diabetes (35). Glucose autoxidation and protein glycation both are processes that are accelerated by high glucose and produce superoxide radical or other ROS (36,37). NADPH oxidase has been shown to be stimulated by hyperglycemia in several cell types (38,39), and its mRNA in endothelial cells is induced sevenfold by high glucose (39). High glucose can turn on NADPH oxidase by de novo synthesis of diacylglycerol (40), which activates PKC, which in turn can activate NAD(P)H oxidase by phosphorylation of p47(phox) (41).

The response of OVE26 cardiomyocytes to high glucose was similar to their response to angiotensin II. Glucose, like angiotensin II, increased ROS levels only in diabetic cardiomyocytes, and in both cases the response was prevented by DPI, MT overexpression, and losartan. This similarity suggests that high glucose acts via angiotensin II or that high glucose requires the simultaneous activation of the angiotensin II system. That losartan and DPI blocked the high glucose response suggests involvement of NADPH oxidase. However, the DPI results cannot be

considered a definitive indication for the involvement of NADPH oxidase, because DPI inhibits other flavoprotein-containing enzymes that may play a role in ROS production. This includes inhibition of complex II of the mitochondrial electron transport chain.

In summary, our data demonstrate that 5 months of diabetes resulted in OVE26 cardiomyocytes with reduced mechanical performance and slow intracellular Ca^{2+} clearing. Permanent antioxidant treatment by MT overexpression prevents these defects. OVE26 myocytes exhibited a significantly greater ROS response to high glucose or angiotensin II, and this was also prevented by MT overexpression. Acute treatment with DPI or losartan blocked the enhanced diabetic ROS production, suggesting that high glucose requires angiotensin II activity and that ROS are produced by a flavoprotein-containing enzyme. Chronic ROS elevation in diabetic cardiomyocytes damages contractility, impairs calcium handling, and may predispose the myocyte to produce greater levels of ROS.

ACKNOWLEDGMENTS

REFERENCES

1. Jaffe AS, Spadaro JJ, Schechtman K, Roberts R, Geltman EM, Sobel BE: Increased congestive heart failure after myocardial infarction of modest extent in patients with diabetes mellitus. *Am Heart J* 108:31–37, 1984
2. Brown RA, Walsh MF, Ren J: Influence of gender and diabetes on vascular and myocardial contractile function. *Endocr Res* 27:399–408, 2001
3. Belke DD, Larsen TS, Gibbs EM, Severson DL: Altered metabolism causes cardiac dysfunction in perfused hearts from diabetic (db/db) mice. *Am J Physiol Endocrinol Metab* 279:E1104–E1113, 2000
4. Ren J, Sowers JR, Walsh MF, Brown RA: Reduced contractile response to insulin and IGF-I in ventricular myocytes from genetically obese Zucker rats. *Am J Physiol Heart Circ Physiol* 279:H1708–H1714, 2000
5. Fein FS: Diabetic cardiomyopathy. *Diabetes Care* 13:1169–1179, 1990
6. Zarich SW, Nesto RW: Diabetic cardiomyopathy. *Am Heart J* 118:1000–1012, 1989
7. Marra G, Cotroneo P, Pitocco D, Manto A, Di Leo MA, Ruotolo V, Caputo S, Giardina B, Ghirlanda G, Santini SA: Early increase of oxidative stress and reduced antioxidant defenses in patients with uncomplicated type 1 diabetes: a case for gender difference. *Diabetes Care* 25:370–375, 2002
8. Penckofer S, Schwertz D, Florczak K: Oxidative stress and cardiovascular disease in type 2 diabetes: the role of antioxidants and pro-oxidants. *J Cardiovasc Nurs* 16:68–85, 2002
9. Cousins RJ: Absorption, transport, and hepatic metabolism of copper and zinc: special reference to metallothionein and ceruloplasmin. *Physiol Rev* 65:238–309, 1985
10. Sato M, Bremner I: Oxygen free radicals and metallothionein. *Free Radic Biol Med* 14:325–337, 1993
11. Thornalley PJ, Vasak M: Possible role for metallothionein in protection against radiation-induced oxidative stress: kinetics and mechanism of its reaction with superoxide and hydroxyl radicals. *Biochim Biophys Acta* 827:36–44, 1985
12. Matsubara J, Tajima Y, Karasawa M: Promotion of radioresistance by metallothionein induction prior to irradiation. *Environ Res* 43:66–74, 1987
13. Bauman JW, Liu J, Liu YP, Klaassen CD: Increase in metallothionein produced by chemicals that induce oxidative stress. *Toxicol Appl Pharmacol* 110:347–354, 1991
14. Nath R, Kumar D, Li T, Singal PK: Metallothioneins, oxidative stress and the cardiovascular system. *Toxicology* 155:17–26, 2000
15. Chen Y, Saari JT, Kang YJ: Weak antioxidant defenses make the heart a target for damage in copper-deficient rats. *Free Radic Biol Med* 17:529–536, 1994
16. Liang Q, Carlson EC, Donthi RV, Kralik PM, Shen X, Epstein PN: Overexpression of metallothionein reduces diabetic cardiomyopathy. *Diabetes* 51:174–181, 2002
17. Epstein PN, Overbeek PA, Means AR: Calmodulin-induced early-onset diabetes in transgenic mice. *Cell* 58:1067–1073, 1989
18. Kang YJ, Chen Y, Yu A, Voss-McCowan M, Epstein PN: Overexpression of metallothionein in the heart of transgenic mice suppresses doxorubicin cardiotoxicity. *J Clin Invest* 100:1501–1506, 1997
19. Overbeek PA, Aguilar-Cordova E, Hanten G, Schaffner DL, Patel P, Lebovitz RM, Lieberman MW: Coinjection strategy for visual identification of transgenic mice. *Transgenic Res* 1:31–37, 1991
20. Kajstura J, Fiordaliso F, Andreoli AM, Li B, Chimenti S, Medow MS, Limana F, Nadal-Ginard B, Leri A, Anversa P: IGF-1 overexpression inhibits the development of diabetic cardiomyopathy and angiotensin II-mediated oxidative stress. *Diabetes* 50:1414–1424, 2001
21. Dutta K, Podolin DA, Davidson MB, Davidoff AJ: Cardiomyocyte dysfunction in sucrose-fed rats is associated with insulin resistance. *Diabetes* 50:1186–1192, 2001
22. Brown RA, Filipovich P, Walsh MF, Sowers JR: Influence of sex, diabetes and ethanol on intrinsic contractile performance of isolated rat myocardium. *Basic Res Cardiol* 91:353–360, 1996
23. Allo SN, Lincoln TM, Wilson GL, Green FJ, Watanabe AM, Schaffer SW: Non-insulin-dependent diabetes-induced defects in cardiac cellular calcium regulation. *Am J Physiol* 260:C1165–C1171, 1991
24. Noda N, Hayashi H, Satoh H, Terada H, Hirano M, Kobayashi A, Yamazaki N: Ca2+ transients and cell shortening in diabetic rat ventricular myocytes. *Jpn Circ J* 57:449–457, 1993
25. Mellors LJ, Kotsanas G, Wendt IR: Effects of pyruvate on intracellular Ca2+ regulation in cardiac myocytes from normal and diabetic rats. *Clin Exp Pharmacol Physiol* 26:889–897, 1999
26. Ha T, Kotsanas G, Wendt I: Intracellular Ca2+ and adrenergic responsiveness of cardiac myocytes in streptozotocin-induced diabetes. *Clin Exp Pharmacol Physiol* 26:347–353, 1999
27. Ren J, Dominguez LJ, Sowers JR, Davidoff AJ: Metformin but not glyburide prevents high glucose-induced abnormalities in relaxation and intracellular Ca^{2+} transients in adult rat ventricular myocytes. *Diabetes* 48:2059–2065, 1999
28. Malhotra A, Reich D, Reich D, Nakouzi A, Sanghi V, Geenen DL, Buttrick PM: Experimental diabetes is associated with functional activation of protein kinase C epsilon and phosphorylation of troponin I in the heart, which are prevented by angiotensin II receptor blockade. *Circ Res* 81:1027–1033, 1997
29. Wohaieb SA, Godin DV: Alterations in free radical tissue-defense mechanisms in streptozocin-induced diabetes in rat: effects of insulin treatment. *Diabetes* 36:1014–1018, 1987
30. Nishio Y, Taki H, Hidaka H, Kashiwagi A: Altered NF-kB activity and oxidative stress-related gene expression in cardiovascular tissues of diabetic rats (Abstract). *Diabetes* 46 (Suppl. 1):A206, 1997
31. Nishio Y, Kashiwagi A, Taki H, Shinozaki K, Maeno Y, Kojima H, Maegawa H, Haneda M, Hidaka H, Yasuda H, Horiike K, Kikkawa R: Altered activities of transcription factors and their related gene expression in cardiac tissues of diabetic rats. *Diabetes* 47:1318–1325, 1998
32. Kaul N, Siveski-Iliskovic N, Hill M, Khaper N, Seneviratne C, Singal PK: Probucol treatment reverses antioxidant and functional deficit in diabetic cardiomyopathy. *Mol Cell Biochem* 160–161:283–288, 1996
33. Bendall JK, Cave AC, Heymes C, Gall N, Shah AM: Pivotal role of a gp91(phox)-containing NADPH oxidase in angiotensin II- induced cardiac hypertrophy in mice. *Circulation* 105:293–296, 2002
34. Korshunov SS, Skulachev VP, Starkov AA: High protonic potential actuates a mechanism of production of reactive oxygen species in mitochondria. *FEBS Lett* 416:15–18, 1997
35. Nishikawa T, Edelstein D, Du XL, Yamagishi S, Matsumura T, Kaneda Y, Yorek MA, Beebe D, Oates PJ, Hammes HP, Giardino I, Brownlee M: Normalizing mitochondrial superoxide production blocks three pathways of hyperglycaemic damage. *Nature* 404:787–790, 2000
36. Gillery P, Monboisse JC, Maquart FX, Borel JP: Glycation of proteins as a source of superoxide. *Diabete Metab* 14:25–30, 1988
37. Hunt JV, Dean RT, Wolff SP: Hydroxyl radical production and autoxidative glycosylation: glucose autoxidation as the cause of protein damage in the experimental glycation model of diabetes mellitus and ageing. *Biochem J* 256:205–212, 1988
38. Craven PA, Phillips SL, Melhem MF, Liachenko J, DeRubertis FR: Overexpression of manganese superoxide dismutase suppresses increases in collagen accumulation induced by culture of mesangial cells in high-media glucose. *Metabolism* 50:1043–1048, 2001
39. Hink U, Li H, Mollnau H, Oelze M, Matheis E, Hartmann M, Skatchkov M, Thaiss F, Stahl RA, Warnholtz A, Meinertz T, Griendling K, Harrison DG, Forstermann U, Munzel T: Mechanisms underlying endothelial dysfunction in diabetes mellitus. *Circ Res* 88:E14–E22, 2001
40. Inoguchi T, Li P, Umeda F, Yu HY, Kakimoto M, Imamura M, Aoki T, Etoh T, Hashimoto T, Naruse M, Sano H, Utsumi H, Nawata H: High glucose

level and free fatty acid stimulate reactive oxygen species production through protein kinase C-dependent activation of NAD(P)H oxidase in cultured vascular cells. *Diabetes* 49:1939–1945, 2000

41. Swain SD, Helgerson SL, Davis AR, Nelson LK, Quinn MT: Analysis of activation-induced conformational changes in p47phox using tryptophan fluorescence spectroscopy. *J Biol Chem* 272:29502–29510, 1997